PNAS RESEARCH ARTICLE | NEUROSCIENCE

Coordinated NADPH oxidase/hydrogen peroxide functions regulate cutaneous sensory axon de- and regeneration

Antonio Cadiz Diaz[a,1], Natalie A. Schmidt[a,1], Mamiko Yamazaki[b,1], Chia-Jung Hsieh[a], Thomas S. Lisse[a,c], and Sandra Rieger[a,c,2]

Edited by Utpal Banerjee, University of California, Los Angeles, CA; received September 15, 2021; accepted March 30, 2022

Tissue wounding induces cutaneous sensory axon regeneration via hydrogen peroxide (H_2O_2) that is produced by the epithelial NADPH oxidase, Duox1. Sciatic nerve injury instead induces axon regeneration through neuronal uptake of the NADPH oxidase, Nox2, from macrophages. We therefore reasoned that the tissue environment in which axons are damaged stimulates distinct regenerative mechanisms. Here, we show that cutaneous axon regeneration induced by tissue wounding depends on both neuronal and keratinocyte-specific mechanisms involving H_2O_2 signaling. Genetic depletion of H_2O_2 in sensory neurons abolishes axon regeneration, whereas keratinocyte-specific H_2O_2 depletion promotes axonal repulsion, a phenotype mirrored in *duox1* mutants. Intriguingly, *cyba* mutants, deficient in the essential Nox subunit, p22Phox, retain limited axon regenerative capacity but display delayed Wallerian degeneration and axonal fusion, observed so far only in invertebrates. We further show that keratinocyte-specific oxidation of the epidermal growth factor receptor (EGFR) at a conserved cysteine thiol (C797) serves as an attractive cue for regenerating axons, leading to EGFR-dependent localized epidermal matrix remodeling via the matrix-metalloproteinase, MMP-13. Therefore, wound-induced cutaneous axon de- and regeneration depend on the coordinated functions of NADPH oxidases mediating distinct processes following injury.

axon regeneration | axon fusion | hydrogen peroxide | EGFR | Wallerian degeneration

Under conditions of injury, H_2O_2 is produced by a family of NADPH oxidases, Duox and Nox, which are located in the plasma membrane and other cellular compartments (1–3) (*SI Appendix*, Fig. S1). These enzymes catalyze the transfer of electrons from NADPH to molecular oxygen, thereby producing $NADP^+$ and superoxide (O_2^-). In a second reaction, O_2^- is converted into H_2O_2 either directly by Duox1/2 (4) and Nox4 (5), or indirectly by the Nox cofactor, superoxide dismutase (6, 7). Plasma membrane-generated H_2O is secreted into the extracellular space from where it diffuses over relatively short distances and enters nearby cells via aquaporins (4, 8). Intracellular H_2O_2 is rapidly utilized by intermediary peroxiredoxins for protein thiol oxidation (9–11), or scavenged by antioxidant complexes (12, 13), thus largely limiting H_2O_2 signaling to juxtamembrane regions within cells.

Nerve lesion experiments in mice combined with dorsal root ganglion (DRG) neuron culture assays demonstrated that macrophage-derived Nox2 is incorporated into DRG axons at the lesion site through exosomal transfer, leading to retrograde transport and neurite outgrowth via nuclear oxidative H_2O_2-dependent mechanisms (14). Notable differences in axon regeneration outcomes have been reported after nerve lesions versus cutaneous injuries. For example, nerve lesions stimulate incomplete regeneration whereby the epidermis remains largely devoid of regenerating axons (15, 16). In contrast, cutaneous injury promotes hyperinnervation of both the dermis and epidermis by cutaneous axons (17–20). Thus, the environment profoundly influences regeneration outcomes. Given the production of H_2O_2 in wound epidermal keratinocytes, we hypothesized that cutaneous injury stimulates axon regeneration through distinct H_2O_2 signaling mechanisms compared with immune cell-dependent repair of nerve lesions. Consistently, we previously showed that innate immune cells are dispensable for cutaneous sensory axon regeneration (21). We demonstrate here that H_2O_2 is required for axon regeneration in both neurons and keratinocytes. We identified via RNA-sequencing (RNA-seq) that the epidermal growth factor receptor (EGFR) is one of the major H_2O_2 targets in keratinocytes and that EGFR oxidation at Cys797 is required for axonal reinnervation of the epidermis involving MMP-13–dependent matrix remodeling. The EGFR has been implicated in a variety of wound-healing functions, including proliferation and stimulation of migration of epidermal keratinocytes, fibroblasts, and endothelial cells under healthy and pathological conditions (22–25). Our study provides evidence for a previously unknown function in promoting wound-epidermal reinnervation by cutaneous axons.

Significance

Cutaneous wound healing depends on axon reinnervation of the skin, yet the mechanisms remain largely elusive because of the lack of suitable models allowing for analyzing tissue interactions in intact organisms. To address this, we utilized zebrafish time-lapse imaging and show a dual role for NADPH oxidases in axon de- and regeneration. Duox1-dependent hydrogen peroxide formation and oxidation of the epidermal growth factor receptor are essential for epidermal reinnervation via matrix remodeling. In contrast, Nox enzymes participate in axon degeneration, whereby loss of a subunit required for Nox1-4 activation, p22Phox, delays Wallerian degeneration and promotes axonal fusion. These findings could aid in therapeutic development for patients with wound healing and axon regeneration defects or in the prevention of axon degeneration.

Author contributions: N.A.S., M.Y., T.S.L., and S.R. designed research; A.C.D., N.A.S., M.Y., C.-J.H., T.S.L., and S.R. performed research; A.C.D., N.A.S., M.Y., T.S.L., and S.R. contributed new reagents/analytic tools; A.C.D., N.A.S., M.Y., C.-J.H., T.S.L., and S.R. analyzed data; S.R. edited the original submission and wrote the paper; A.C.D. edited the paper; and S.R. edited the revised paper.

The authors declare no competing interest.

This article is a PNAS Direct Submission.

[1]A.C.D., N.A.S., and M.Y. contributed equally to this work.

[2]To whom correspondence may be addressed. Email: srieger@miami.edu.

This article contains supporting information online at http://www.pnas.org/lookup/suppl/doi:10.1073/pnas.2115009119/-/DCSupplemental.

Published July 19, 2022.

Results

Tissue Injury Induces Cysteine Sulfenylation Near the Wound. H_2O_2 functions as a second messenger by oxidizing cysteine thiols, leading to sulfenic acid formation (sulfenylation). Sulfenylation may promote intramolecular disulfide bond formation that can either activate or inactivate enzymes, such as kinases and phosphatases (26, 27). To determine the role of sulfenylation in cutaneous sensory axon regeneration, we sought to assess the extent to which sulfenylation occurs following injury, and whether inhibition of oxidation-dependent metabolic thiol conversion influences axon regeneration (Fig. 1*A*). Coupling an alkyne-tagged dimedone analog (DYn-2) (28) with oxidized cysteine thiol allowed for click chemistry-mediated fluorescent detection of sulfenylated proteins ~30 min postinjury (mpi) in the caudal fins of 3-d postfertilization (dpf) zebrafish when

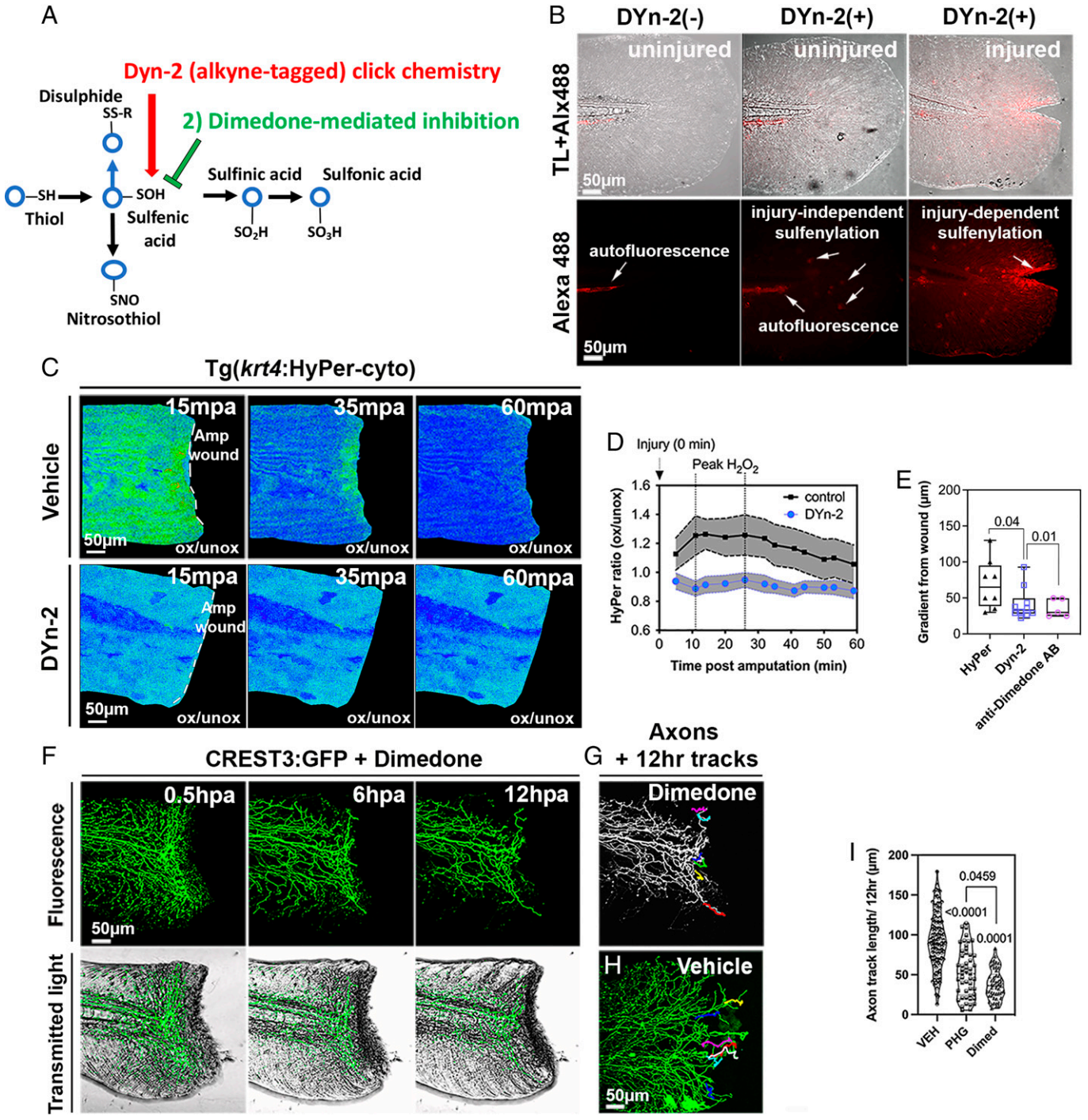

Fig. 1. Cysteine oxidation is essential for cutaneous sensory axon regeneration at 3 dpf. (*A*) Model for thiol oxidation reactions and targeting of sulfenic acid with dimedone or alkyne-tagged DYn-2. (*B*) Click chemistry with DYn-2 detects sulfenylated protein gradient (red) at 30 mpi, but not in injured DYn-$2^{(-)}$ or uninjured DYn-$2^{(+)}$ animals. (*C* and *D*) Time-lapse imaging of Tg(*krt4*:HyPer) fish for 60 min following amputation reveals peak oxidation at ~15 to 30 mpa, whereas oxidation is largely prevented in DYn-2–treated animals ($n = 10$ animals per group, two-way ANOVA: $P < 0.0001$ for vehicle vs. DYn-2). (*E*) Mean gradient width from wound is greatest with HyPer detection compared to DYn-2 and dimedone staining ($n = 7$, 8, and 4 animals, respectively). (*F–H*) Time-lapse imaging of sensory neurons mosaically expressing CREST3:Gal4VP16_14xUAS_GFP shows impaired axon regeneration with dimedone (*F* and *G*) compared to vehicle controls (*H*). (*I*) Quantification shows reduced regeneration also in the presence of the antioxidant, PHG ($n = 10$ animals per group). One-way ANOVA and Tukey's (*E*) or Bonferroni's (*I*) posttest was used. Significance above columns compares to vehicle group.

sensory neurons have terminally differentiated. The DYn-2–AlexaFluor-561 staining largely resembled the previously shown H_2O_2 gradient formed upon skin wounding, for which a peak was detected ∼20 mpi when using ratiometric HyPer imaging (29) (Fig. 1*B*). Sulfenylation detection was specific since zebrafish that did not undergo click chemistry showed merely autofluorescence in the ventral notochord region, which is rich in vasculature (30). In contrast, uninjured control animals subjected to click chemistry displayed scattered fluorescent cells throughout the fin, which could be apoptotic cells, or a different cell type that naturally possesses higher oxidation levels. Indeed, more of these scattered cells appeared throughout the fin following wounding, in addition to the sulfenylation gradient, suggesting that these could be immune cells (29, 31).

We next hypothesized that the main function of sulfenylation is to contribute to intramolecular disulfide bond formation in proteins, as this has been shown to activate kinases and inactivate phosphatases, promoting protein phosphorylation within cells (32). If true, we expected to see reduced HyPer emission in the oxidized channel (516 nm) upon DYn-2 treatment due to the prevention of intramolecular disulfide bond formation necessary for HyPer emission shifts (33). At 3 dpf, epidermal keratinocytes in zebrafish express *krt4* in both epidermal layers (*SI Appendix*, Fig. S2). We therefore used our Tg(*krt4*:HyPer-cyto) transgenic animals (34) to monitor HyPer oxidation in the presence of dimethyl sulfoxide (DMSO) vehicle (0.1%) and DYn-2. The average peak oxidation in the controls lasted between ∼10 and 30 min postamputation (mpa), whereas this peak was largely abolished upon pretreatment with 10 μM DYn-2 (Fig. 1*C* and *D* and Movies S1 and S2). This confirmed that sulfenylation contributes to intramolecular disulfide bond formation at the wound. Previous studies utilizing HyPer mRNA suggested the existence of an H_2O_2 gradient emanating from the wound (29). Although we also observed HyPer gradients extending up to ∼150 μm from the wound margin, the extent was highly variable among animals. HyPer gradients were more distant than the sulfenylation gradients detected with click chemistry and when using anti-dimedone antibody staining (HyPer: 69.4 ± 12.2 μm vs. DYn-2: 41.4 ± 6.9 μm vs. dimedone: 35.7 ± 5.7 μm, SEM) (Fig. 1*E*). In general, HyPer ratios in keratinocytes were much lower than those previously reported using ubiquitous HyPer mRNA (29), suggesting that H_2O_2 diffuses into other cell types at the wound, possibly mesenchymal cells (35) or immune cells (29, 31, 36).

To determine if thiol oxidation is essential for cutaneous axon regeneration, we treated live fish injected with *CREST3*:GFP to label cutaneous axons with nonalkyne-tagged dimedone (37). Dimedone was previously shown to impair T cell activation and proliferation (38), indicating that sulfenylation also plays a role in these processes. Following 0.5-h treatment with either vehicle (0.15% DMSO) or 1.5 mM dimedone, axon regeneration was monitored in the caudal fin for 12 h using time-lapse imaging. The antioxidant phloroglucinol (25 μM PHG) (39) was used as positive control. Compared to vehicle-treated animals, axon regeneration was impaired with both PHG and dimedone (vehicle: 92.5 ± 3.3 μm/12 h vs. PHG: 52.5 ± 4.3 μm/12 h vs. dimedone: 37.9 ± 2.7 μm/12 h, SEM) (Fig. 1*F*–*I* and Movies S3 and S4), indicating that oxidation and sulfenic acid formation are essential for cutaneous axon regeneration, consistent with H_2O_2 second messenger functions.

HyPer Imaging Reveals H_2O_2 Diffusion into Axons. We previously demonstrated that axon regeneration was impaired in *duox1*-morpholino injected animals, yet, transplantation of sensory neurons from *duox1* morphants into wild-type hosts did not perturb regeneration (21), suggesting neuron-extrinsic functions for Duox1/H_2O_2 in axon regeneration, consistent with the epithelial Duox expression (4, 40–43). To further investigate the cell type-specificity of H_2O_2, we used HyPer imaging in 3-dpf animals transiently injected with *CREST3*:HyPer to detect H_2O_2 in sensory axons. We expected to detect HyPer oxidation in axon branches near the wound if H_2O diffuses from keratinocytes into axons. Indeed, localized HyPer oxidation in cutaneous axon branches near the wound was observed ∼30 to 35 mpi, slightly later than the oxidation peak observed in keratinocytes (Fig. 2*A*–*C*). Addition of 0.01% H_2O_2 to uninjured animals transiently increased axonal HyPer oxidation within ∼3 to 5 min (Fig. 2*D*), validating our detection method. Interestingly, in addition to dynamic axonal fluorescent puncta near the injury site, we noticed sustained oxidation in stable puncta within the primary axon branch and in the soma (Fig. 2*A* and *B*). Given that cytoplasmic H_2O_2 diffusion is mostly restricted to juxtamembrane regions, these puncta may represent sites of mitochondrial and nuclear H_2O_2 production leaking into the cytoplasm (44), which may directly or indirectly contribute to axon de- and regeneration (3, 5, 14). To substantiate that epidermal Duox mediates H_2O_2 diffusion into axons, we assessed neuronal HyPer oxidation in homozygous *duox1*^{sa9892} mutants, which carry a mutation leading to premature chain termination after amino acid 945. This eliminates the calcium-binding EF hand motifs and FAD/nicotinamide adenine dinucleotide (NAD) binding domains necessary to produce superoxide and H_2O_2 (*SI Appendix*, Fig. S1*A*). Homozygous *duox1* mutants are viable until ∼5 dpf and appear wild-type–like. On rare occasions, homozygous female fish survived to adulthood but were sterile. HyPer oxidation in *duox1*$^{(-/-)}$ was absent in axon branches near the wound (Fig. 2*C* and *D*, *SI Appendix*, Fig. S3*A*, and Movies S5 and S6), as it was absent in keratinocytes (*SI Appendix*, Fig. S3*B*). This indicates that Duox-dependent H_2O_2 diffuses into cutaneous axons where it may participate in oxidation-dependent signaling (Fig. 2*E*).

Genetic H_2O_2 Scavenging in Keratinocytes and Sensory Neurons Contributes to Distinct Axon Regeneration Phenotypes. The presence of H_2O_2 in both keratinocytes and cutaneous sensory axons suggested that H_2O_2 could act in either one or both cell types to stimulate axon regeneration. To assess this in more detail, we genetically scavenged H_2O_2 in sensory neurons and keratinocytes via overexpression of cytoplasmic Glutathione peroxidase 1a (Gpx1a), which converts H_2O_2 into water. We first validated that Gpx1a successfully scavenged H_2O_2 using ratiometric HyPer imaging in keratinocytes (*SI Appendix*, Fig. S3*C*). Overexpression of *gpx1a* under the neuron-specific *CREST3* promoter completely abolished axon regeneration monitored for 12 h, unlike in control fish (control: 180.6 ± 18.7 μm vs. Gpx1a: 27.31 ± 1.21 μm, SEM) (Fig. 3*A* and *B* and Movie S7). This shows that neuron-intrinsic H_2O_2 signaling is essential for cutaneous axon regeneration, consistent with nerve lesion studies (14).

To assess whether H_2O_2 signaling is also essential for axon regeneration in keratinocytes, we overexpressed *gpx1* under the *krt4* promoter (*krt4:Gal4VP16_dtTomato_5xUAS_gpx1a*), together with *CREST3*:LexA_lexAop_GFP to colabel axons. Mosaic expression allowed for genetic manipulation of only a few cells while neighboring, unlabeled cells exhibit wild-type phenotypes. Mosaic expression in zebrafish is observed following plasmid DNA injection and may be the result of degradation of injected DNA to less than one copy per cell during gastrulation (45). Unlike neuronal Gpx1a overexpression leading to impaired axon regeneration, H_2O_2 scavenging in keratinocytes did not impair overall the regenerative capacity of axons but led to axonal retraction

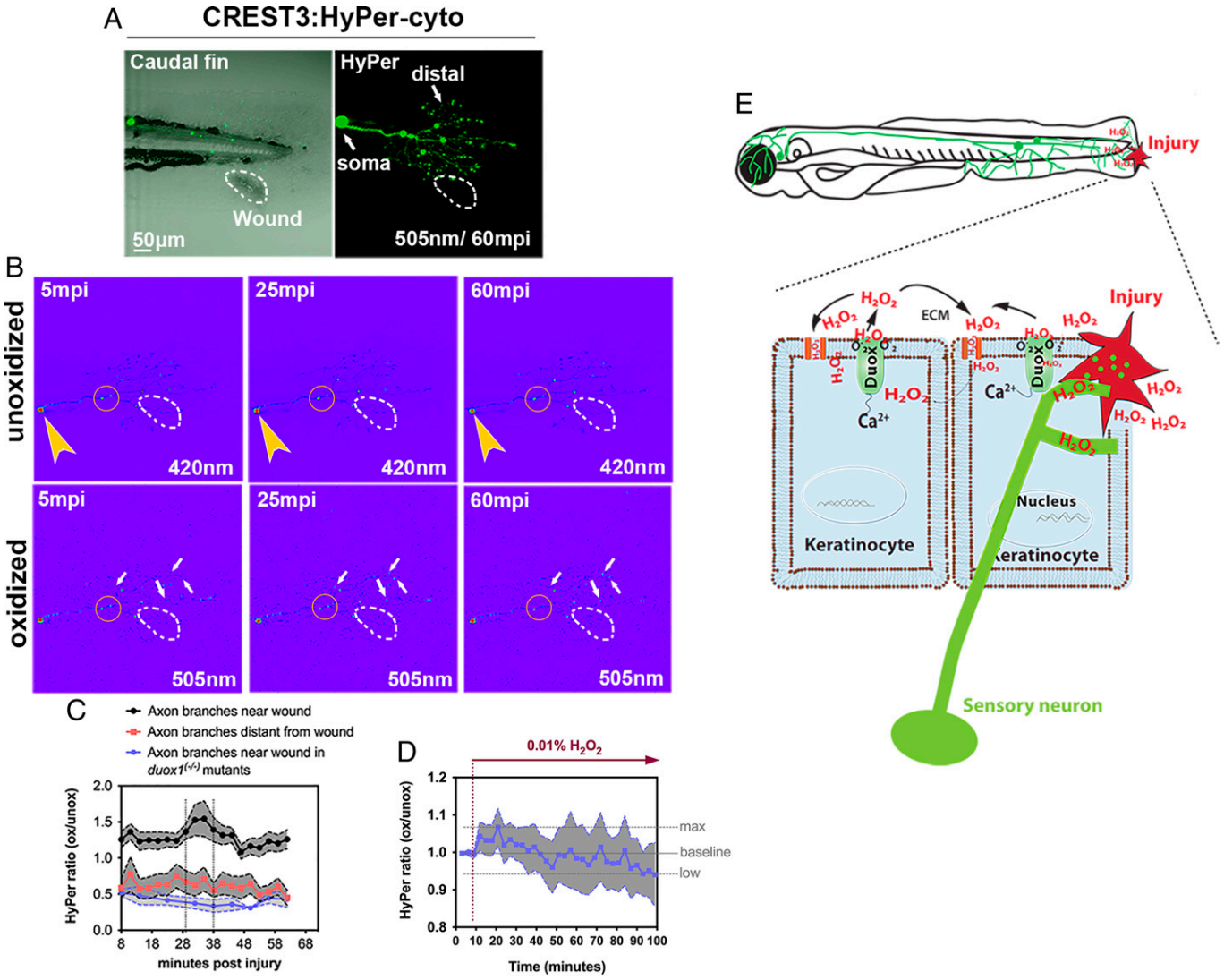

Fig. 2. Thiol oxidation in cutaneous axon branches near the wound. (*A*) HyPer fluorescence in Rohon-Beard neuron innervating the caudal fin. White dotted circle indicates the site of skin wounding. (*B*) Intensity plots show HyPer fluorescence (unoxidized [*Upper*] and oxidized [*Lower*]) in cutaneous axon branches of neuron shown in *A* at 5, 25, and 60 mpi. White-dotted circle indicates the wound site. White arrows point to small HyPer puncta in branches near the wound that become oxidized. Note the presence of stable oxidized HyPer fluorescence in the soma (yellow arrowheads) and primary branch (small red circle). (*C*) HyPer ratios in axonal puncta near (<150 μm) and distant from (>150 μm) the wound. The oxidation peak in puncta near the wound is detected ~35 mpi but is absent in distant branches and branches near the wound in *duox1*$^{(-/-)}$ (n = 3 animals per group). (*D*) HyPer detection upon H_2O_2 addition to uninjured zebrafish within ~ to 5 min (n = 6 animals). (*E*) Schematic representation of Duox-dependent H_2O_2 secretion and cytoplasmic uptake into keratinocytes and cutaneous axons.

upon establishing contact with H_2O_2-deficient cells (control *krt4:Gal4VP16_dtTomato*: 167.7 ± 12.7 μm vs. *krt4:gpx1a+CREST3*:GFP distant: 150.3 ± 10.8 μm vs. *krt4:gpx1a+CREST3*:GFP contact: −50.2 ± 11.1 μm [retraction], SEM) (Fig. 3*C–E* and Movie S8). This indicates that H_2O_2 is essential for axon regeneration in both neurons and keratinocytes, but the signaling functions differ. Neurons require H_2O_2 for axonal outgrowth whereas keratinocytes promote cutaneous reinnervation, which may both underlie distinct molecular mechanisms.

Given the known hormetic functions of H_2O_2, we speculated that axon regeneration is also impaired when H_2O_2 concentrations are elevated above physiological levels. To test this, we treated 3-dpf zebrafish with 0.3% H_2O_2, which is 30-fold higher than the maximum tolerated H_2O_2 concentration in zebrafish when continuosuly treated for 12 h (21). Under these conditions, cutaneous axons did not regenerate following amputation, and both uninjured and amputated fish did not survive for more than 4 to 5 h (*SI Appendix*, Fig. S4 and Movie S9). Thus, consistent with previous observations, our data indicate that tightly regulated H_2O_2 concentrations are critical for neuronal survival and regeneration.

Lyn Kinase Is Not Involved in Cutaneous Axon Regeneration. The Src family kinase, Lyn, is a downstream effector of H_2O_2 in zebrafish, and its activation is induced by oxidation-dependent intramolecular disulfide bond formation, which stimulates the migration of neutrophils toward the wound (31). Besides neutrophiles, Lyn expression has been reported in nonhematopoietic tissues (31, 46, 47), including the nervous system (48). To determine whether Lyn also plays a role in cutaneous axon regeneration, we used a validated morpholino (31), which showed that axon regeneration was comparable to wild-type amputated fish (wild-type 12-h growth: 85.8 ± 2.5 μm vs. *lyn*-morpholino: 82.81 ± 6.9 μm, SEM) (*SI Appendix*, Fig. S5 and Movie S10), indicating that Lyn is nonessential. We further assessed whether NF-κB, a downstream target of Src tyrosine kinases (49) that is regulated by H_2O_2 (50) is involved in cutaneous axon regeneration, but pharmacological inhibition of NF-κB did not impair regeneration (81.11 ± 4.8 μm, SEM). Consistent with our previous findings that immune cell-deficient zebrafish *cloche* mutants regenerate their axons (21), and reported upstream functions for neurotrophic signals in wound-induced inflammation (51), these

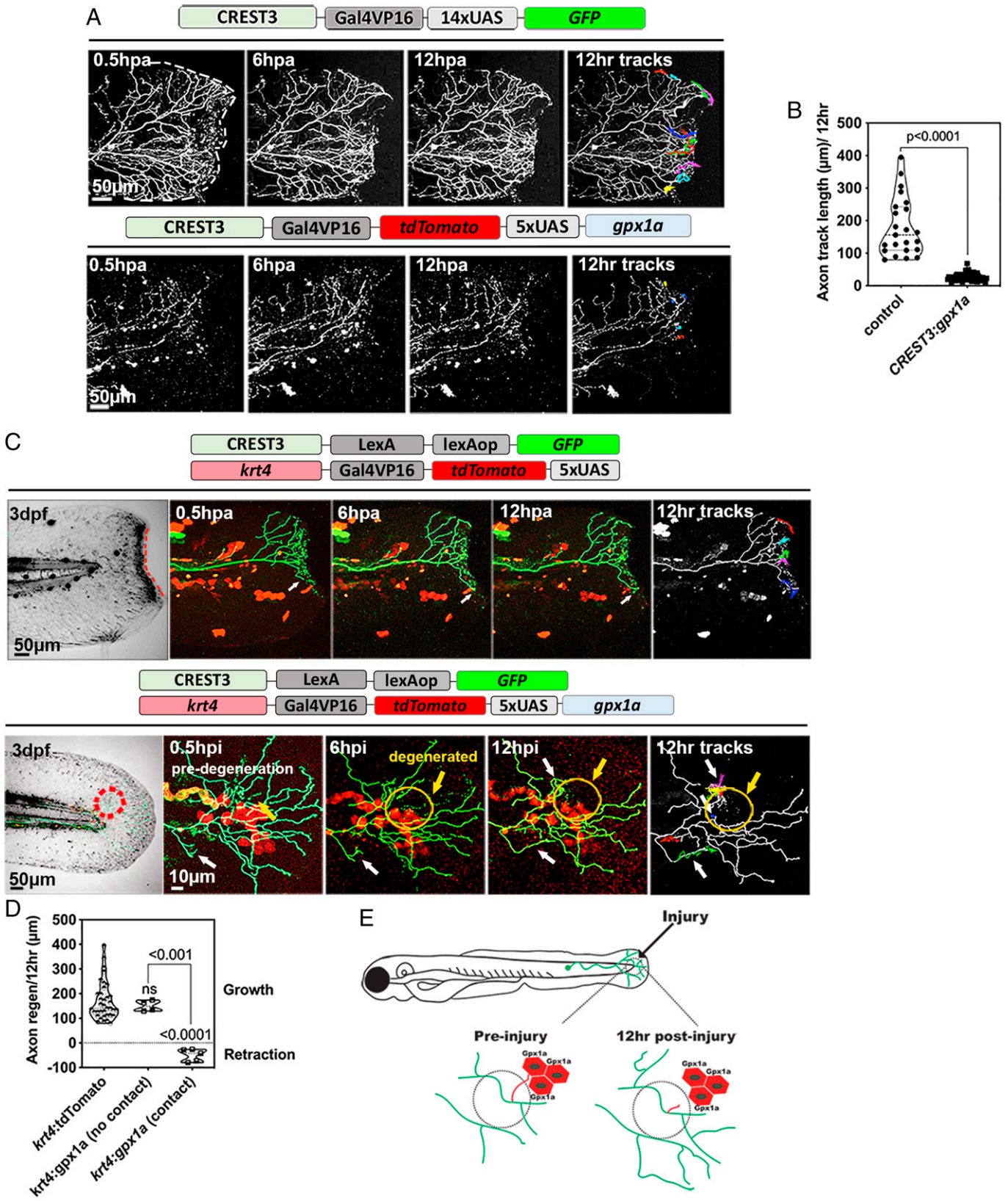

Fig. 3. Neuronal and keratinocyte specific H_2O_2 depletion induces distinct axon regeneration phenotypes. (*A* and *B*) Overexpression of *gpx1a* in sensory neurons abolishes axon regeneration, confirmed upon 12-h tracking (colored lines). (*B*). Quantification of *A* (control: $n = 4$; *CREST3:gpx1a:* $n = 5$ animals). (*C*) Coexpression of *krt4*:Gal4VP16_tdTomato_5xUAS with CREST3:LexA_lexAop_GFP (*Upper*) shows axon regeneration distant from the wound (white arrow points to branch that regenerates upon contact with tdTomato$^+$ keratinocyte). (*Lower*) Axon regeneration does not occur and branches retract when in contact with keratinocytes expressing *krt4*:Gal4VP16_tdTomato_5xUAS_*gpx1a* (yellow circle; yellow arrow points to degenerated axon branches, white arrow points to distant regenerating branch). (*D*) Axon track length is similar between injured branches in the controls and distant branches, while branches in contact with tdTomato_*gpx1*$^+$ keratinocytes retract (left to right: $n = 6$, 5, and 5 animals). Statistical comparisons use ANOVA and Sidak's multiple comparisons test. Significance above columns compares to the control column. Bracket indicates alternative comparison. (*E*) Schematic of observations shown in *C* and *D*.

results suggest that early inflammatory signals are not necessary for cutaneous axon regeneration.

Loss of Duox1 Leads to Axonal Repulsion, whereas Loss of p22Phox Delays Wallerian Degeneration and Promotes End-Joining of Severed Axon Branches. Given the role of Duox in H_2O_2 diffusion into sensory neurons, we wanted to identify if Duox1 and other Nox enzymes are critical for cutaneous axon regeneration. As previously shown in *duox1* morphants, homozygous *duox1* mutants also did not regenerate their axons following caudal fin amputation, and similar to keratinocyte-specific *gpx1a* overexpression, axon branch tips retracted over the course of 12 h (wild-type uninjured: 8.33 ± 1.4 μm [retraction] vs. wild-type amputated: 91.52 ± 3.0 μm [growth] vs. *duox1*^{sa9892} amputated: −35.0 ± 2.8 μm [retraction] vs. *duox1*-morpholino amputated: −36.5 ± 2.1 μm [retraction], SEM) (Fig. 4*A* and *C* and Movie S11).

Amputation studies in zebrafish suggested that *duox1* morphants do not display macrophage migration to the wound (29). Intriguingly, our data show that 62.5% of heterozygous *duox1* fish also lacked wound-directed migration upon caudal fin amputation despite that the migration distance and velocity within the vasculature remained similar to wild-type fish (*SI Appendix*, Fig. S6). This suggests that reduced H_2O_2 concentrations due to the loss of one *duox* allele is sufficient to prevent H_2O_2 sensing in most macrophages.

We next studied the role of Nox enzymes in axon regeneration using the *cyba*^{sa11798} allele, which causes premature chain termination after amino acid 87 in p22Phox (*SI Appendix*, Fig. S1*B* and *C*), preventing Nox activation (6, 52). Homozygous *cyba* fish were viable and maintained breeding capacity as adults. These fish did not show any obvious phenotypes and, unlike the *duox1* mutants, displayed moderate growth and retraction of axons following amputation (*cyba*^{11798} axon growth: 35.86 ± 3.4 μm, SEM) (Fig. 4*B* and *C* and Movie S12), consistent with HyPer oxidation being present in axons near the wound (Fig. 4*D*). Intriguingly, *cyba* mutants displayed delayed Wallerian degeneration that mimicked the Wld^S phenotype (53), whereby the lag phase (the period between amputation and axon fragmentation onset) was delayed by several hours in ∼30% of cutaneous axon branches. The lag phase typically lasts between 45 to 100 min, depending on the type of injury (54), but in *cyba* mutants, fragmentation onset was sometimes delayed ∼5 to 6 h (Fig. 4*E* and *F* and Movies S13 and S14), Moreover, ∼40 to 50% of axon branches in the *cyba* mutants did not show any fragmentation, which compared to only ∼10% in wild-type fish without fragmentation. This contrasts *duox1* mutants, which displayed massive axon fragmentation and die-back. Even more intriguing was the observation that some severed, but nondegenerating, axon branches in the *cyba* mutants fused with intact proximal branches (Fig. 4*G* and Movie S15), which thus far has only been described in invertebrates (55). Together, these findings indicate that Duox is the primary source of H_2O_2 required for cutaneous axon regeneration, and that Nox enzymes participate in regulated axon degeneration. Since delayed Wallerian degeneration and axonal fusion observed in *cyba* mutants cannot be reproduced by scavenging H_2O_2, it is likely that alternative p22Phox/Nox mechanisms may underlie this process.

Keratinocyte-Specific EGFR Oxidation Is Required for Epidermal Reinnervation. The *duox1* phenotype suggested that H_2O_2 serves as attractive cue in the epidermis, likely through H_2O_2 second messenger functions involving transcriptional and post-transcriptional regulation (56). To assess transcription and translation requirements for cutaneous axon regeneration, we treated 3-dpf fish with the transcription inhibitors, actinomycin-D, 6-mercaptopurine (6-MP), and 5,6-Dichloro-1-β-Ribo-furanosyl benzimidazole (DRB). Surprisingly, 12-h time-lapse imaging following amputation showed that neither actinomycin-D nor 6-MP impaired regeneration. In contrast, the RNA polymerase II inhibitor, DRB, partially decreased regeneration and the translation inhibitor, cycloheximide, most strongly impaired regeneration (DMSO vehicle: 98.8 ± 5.1 μm vs. actinomycin D: 114.4 ± 8.3 μm vs. 6-MP: 96.7 ± 6.7 μm vs. DRB: 63.0 ± 4.9 μm vs. cycloheximide: 36.1 ± 3.9 μm, SEM) (Fig. 5*A*). This suggests that posttranscriptional regulation is prevalent, consistent with local mRNA translation during axon regeneration (57–59).

We next analyzed a previously acquired RNA-seq dataset from zebrafish treated with H_2O_2 (60) to identify upstream regulators of H_2O_2 target genes, using Ingenuity Pathway Analysis software. Upstream regulators of the gene set were identified as H_2O_2 (validating the approach) and the EGF. Both were predicted to coregulate a total of 23 genes, of which 18 were up- and 5 genes down-regulated (Fig. 5*B*, *SI Appendix*, and Dataset S1). Among the most highly up-regulated genes were the matrix-metalloproteinases (MMP), *mmp9* and *mmp10*, *fosl1*, *cyp1a1*, *junb*, *cebpb*, *ctss*, *dnajb1*, and *igfbp1*. Down-regulated genes represented *elf3*, *cyr61*, *jund*, *serpinh1*, and *klf4*. For several genes, interactions with either H_2O_2 or EGF, or both, had been validated, including *mmp10*, *fosl1*, *atf3*, *cyp1a1*, *epha2*, *hmox1*, and *odc1*.

The EGFR has been implicated in developmental innervation of the epidermis by DRG neurons in mice where its targeted deletion within keratinocytes led to hyperinnervation and disorganization of cutaneous axon branch patterns in the epidermis (61). We therefore assessed the effects of pharmacological EGFR inhibition on cutaneous axon regeneration in zebrafish following amputation during and after developmental innervation of the skin (1 dpf vs. 3 dpf). Tracking regenerating axons following amputation in zebrafish treated with EGFR inhibitor and Erbstatin (both inhibiting EGFR phosphorylation) (62, 63) at 1 dpf phenocopied the epidermal hyperinnervation observed in mice for the EGFR inhibitor, whereas Erbstatin slightly reduced regeneration (vehicle: 101.0 ± 5.0 μm vs. 9 μM EGFR inhibitor: 141.1 ± 6.9 μm vs. 10 μM Erbstatin: 85.8 ± 3.9 μm, SEM) (Fig. 5*C*). Interestingly, EGFR inhibition at 3 dpf significantly reduced axon regeneration when using various EGFR inhibitors compared with the controls (vehicle: 98.8 ± 5.1 μm vs. 8 μM EGFR inhibitor: 47.5 ± 4.4 μm vs. 9 μM EGFR inhibitor: 36.4 ± 3.6 μm vs. Erbstatin: 49.0 ± 4.4 μm vs. 10 μM Lavendustin A: 55.2 ± 6.6 μm vs. Tyrphostin 23: 46.3 ± 5.4 μm, SEM) (Fig. 5*C*). Thus, EGFR requirements during developmental innervation of the epidermis are distinct from those during postinnervation stages.

In the A431 human cancer cell line, EGFR oxidation at C797 leads to enhanced kinase activity in the presence of EGF (28). This cysteine residue is conserved in zebrafish EGFR, suggesting a critical function. We therefore generated an EGFR(C797A) dominant-negative variant fused to GFP expressed in basal keratinocytes [*tp63*:EGFR(C797A-GFP)]. Both this variant and a wild-type zebrafish EGFR-GFP control plasmid were transfected into human keratinocytes (HaCaT) to assess their localization. The wtEGFR-GFP was localized to the plasma membrane, whereas EGFR(C797A) showed increased cytoplasmic localization, confirmed by a reduced membrane:cytoplasmic ratio [wtEGFR-GFP: 1.8 ± 0.1 vs. *tp63*:EGFR (C797A)-GFP: 1.2 ± 0.18, SEM] (Fig. 5*D* and *E*). Increased EGFR internalization has also been described upon treating nonsmall-cell lung cancer cells with the EGFR inhibitor, Erlotinib (64), suggesting that internalization of zfEGFR(C797A) is likely

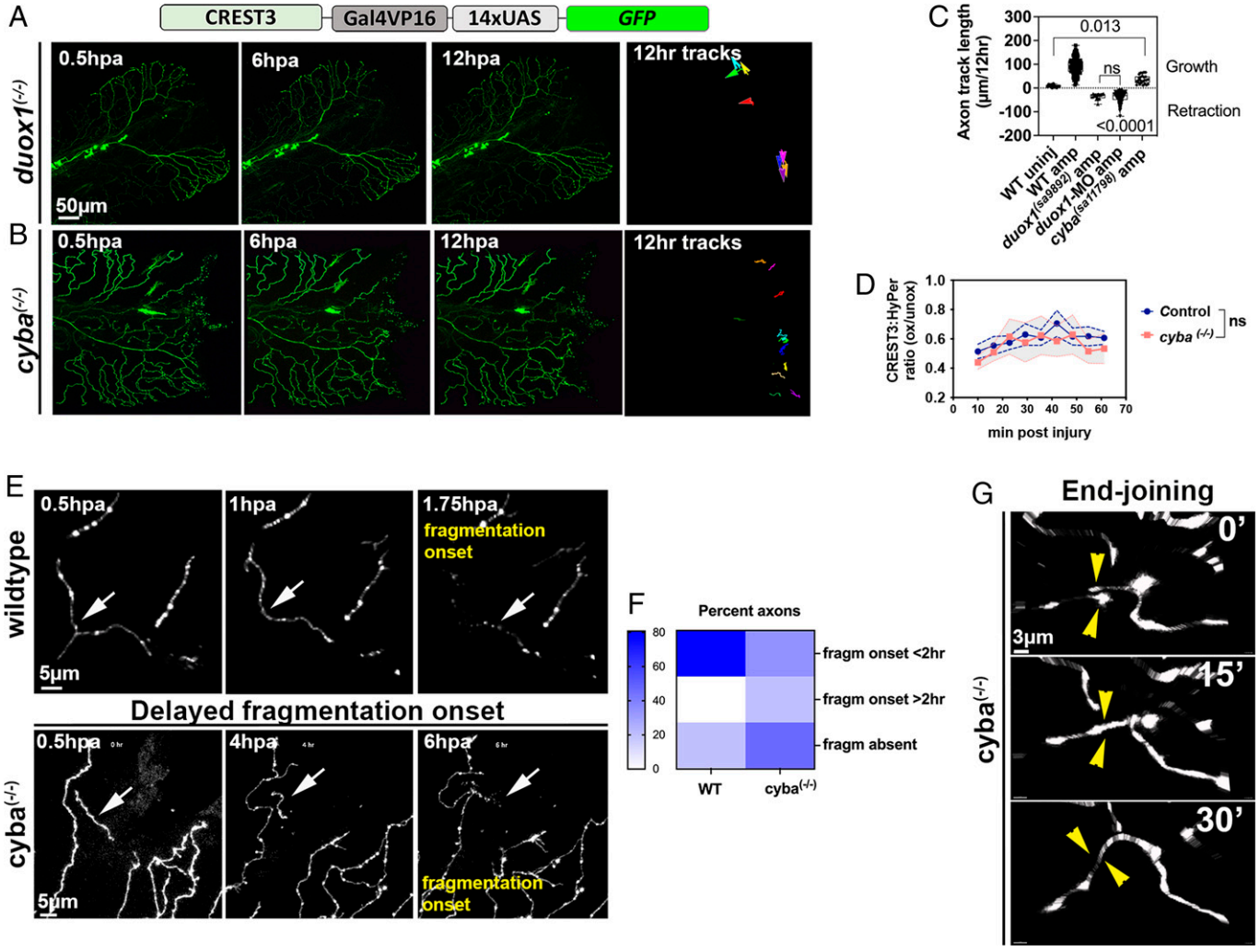

Fig. 4. Phenotypic differences between *duox1*$^{(-/-)}$ and *cyba*$^{(-/-)}$ mutants. (*A*) Time-lapse imaging of a 3dpf *duox1*$^{(-/-)}$ mutant shows largely retraction of axon branches at the amputation wound, as indicated by 12-h colored tracks/arrows. (*B*) A *cyba*$^{(-/-)}$ mutant retains some regenerative capacity, as indicated by 12-h tracks. (*C*) Cutaneous axons retract in *duox1*$^{(-/-)}$ mutants and morphants, whereas *cyba*$^{(-/-)}$ mutants show limited growth, although significantly reduced compared with amputated wild-type fish (left to right: n = 3, 12, 5, 10, and 5 animals, one-way ANOVA, all comparisons are significantly different [$P < 0.0001$] except where indicated otherwise); amp, amputation; MO, morpholino; uninj. uninjured. (*D*) HyPer oxidation measured in axon branches near the amputation wound of control and *cyba*$^{(-/-)}$ mutants reveals similar oxidation increase following injury [n = 3 control, n = 5 *cyba*$^{(-/-)}$ fish]. (*E*) Wallerian degeneration onset in *cyba*$^{(-/-)}$ mutant at ~6 hpa compared with wild-type onset at ~1.75 hpa (arrows). (*F*) Fragmentation onset occurs within 2 hpa in ~80% of wild-type and >2 hpa in ~30% of *cyba*$^{(-/-)}$ fish, whereas ~40% *cyba*$^{(-/-)}$ fish show no fragmentation (wild-type: n = 5; *cyba*$^{(-/-)}$: n = 4, two-way ANOVA, wild-type vs. *cyba*$^{-/-}$: P = 0.002) (*G*) Severed axon branches fuse in a *cyba*$^{(-/-)}$ mutant.

caused by the loss in EGFR activity, consistent with the EGFR activating functions of H_2O_2 (28). We next assessed endogenous EGFR oxidation in HEK001 human keratinocytes (23). DYn-2 treatment followed by click-chemistry pulled down oxidized proteins, which were subsequently probed with anti-EGFR antibody during Western blotting. Antiglutathione peroxidase (GPX), a known oxidation target, was used as positive control (65). Addition of 0.01% H_2O_2 to the cells for 30min resulted in 1.5-fold enrichment in EGFR and 2.8-fold in GPX compared with untreated control cells (Fig. 5*F*), confirming EGFR oxidation in epidermal keratinocytes.

To determine whether EGFR oxidation was critical for cutaneous axon regeneration, we mosaically expressed EGFR(C797A) in keratinocytes coexpressing tdTomato from the same construct, while axons were colabeled with *CREST3*:LexA_lexAop_GFP. Injury followed by 12-h time-lapse imaging showed a phenotype that largely mimicked *gpx1a* overexpression, whereby axon branches contacting EGFR(C797A) keratinocytes retracted upon contact while distal branches of the same neuron regenerated [*krt4*:Gal4VP16_tdTomato+*CREST3*:LexA_lexAop_GFP: 145.1 ± 9.6 µm vs. *krt4*:Gal4VP16_tdTomato_EGFR(C797A)+*CREST3*:LexA_lexAop_GFP distal: 148.4 ± 12.5µm vs. contact: −39.8 ± 9.9 µm (retraction), SEM] (Fig. 5*G* and *H* and Movie S16). Consistently, areas in which EGFR(C797A) keratinocytes were present remained devoid of axons when monitored over the course of 12 h [number of branches/50 µm for *krt4*:tdTomato+*CREST3*:GFP: 0.5 h postamputation (hpa) 14.8 ± 1.36 µm; 6 hpa 12.6 ± 1.36 m; 12 hpa 13.9 ± 0.6 µm vs. *krt4*:tdTomato_EGFR(C797A)+*CREST3*:LexA_lexAop_GFP: 0.5 hpa 13.9 ± 1.3 µm; 6 hpa 8.0 ± 2.8 µm; 12 hpa 8.8 ± 1.3 µm, SEM] (Fig. 5*I*), indicating that EGFR oxidation is critical for epidermal reinnervation. EGFR was shown to coimmunoprecipitate with Nox2 in A431 cancer cells (28), suggesting the possibility of a regulatory feedback mechanism to sustain or inhibit EGFR-dependent reactive oxygen species (ROS) production. To assess this possibility, we measured relative H_2O_2 concentrations in epidermal keratinocytes of amputated Tg(*krt4*:HyPer) fish in the presence and absence of EGFR inhibitor. Compared with controls, pharmacological EGFR inhibition significantly reduced the HyPer oxidation ratios monitored over 60 min (maximal

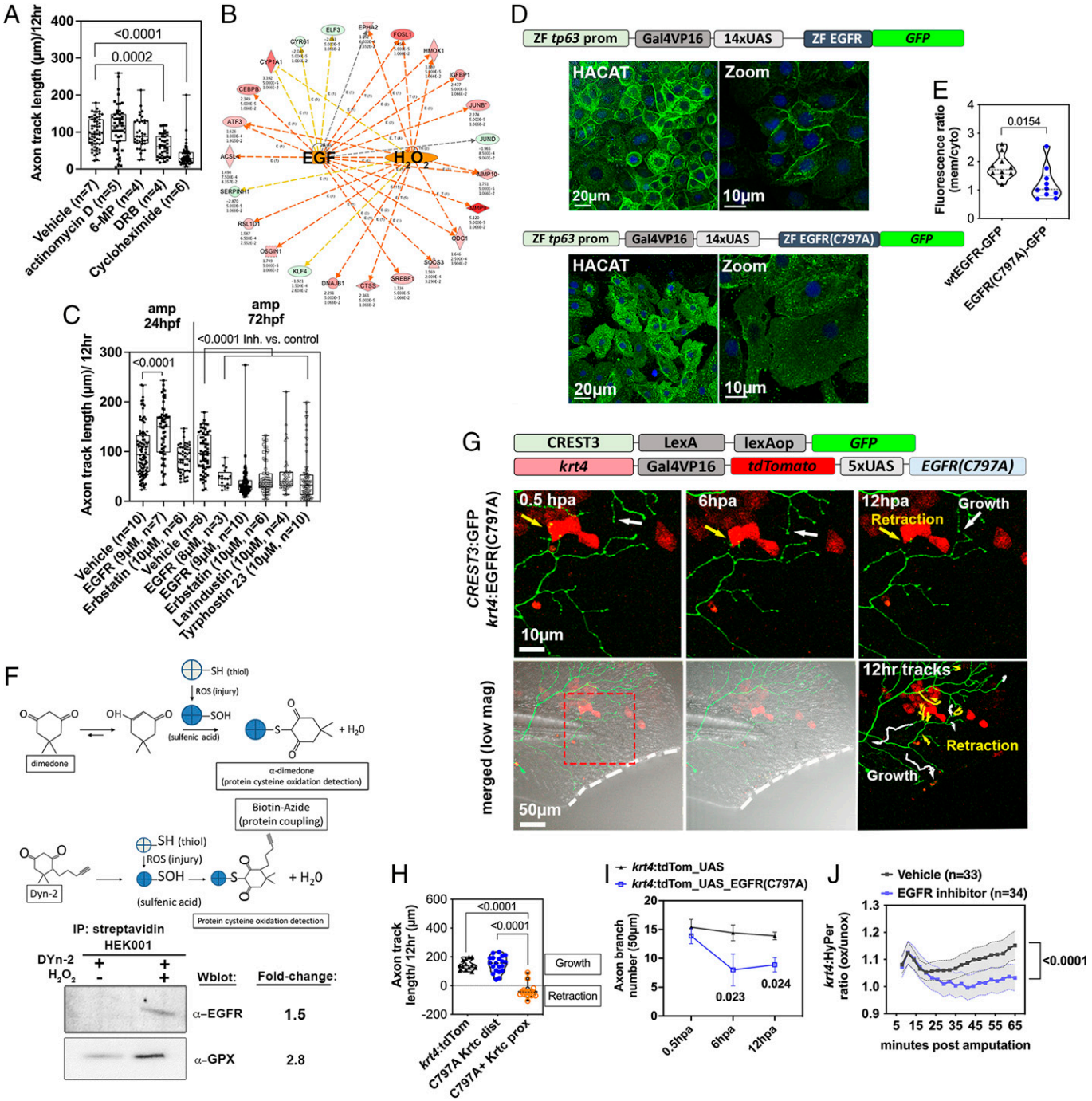

Fig. 5. Keratinocyte-specific oxidation of EGFR-Cys797 promotes axon regeneration. (*A*) The transcription inhibitor, DRB, and the translation inhibitor, cycloheximide, but not actinomycin D and 6-MP, impair axon regeneration in 3-dpf zebrafish. (*B*) Ingenuity Upstream Pathway analysis of RNA-seq data to determine H_2O_2 transcriptional profile in 4-dpf zebrafish shows H_2O_2 and EGF as common upstream regulators of transcriptionally up-regulated (red) and down-regulated (green) genes. (*C*) Antagonistic EGFR functions regulate axon regeneration during (1 dpf) and after (3 dpf) skin innervation by Rohon-Beard neurons. (*D*) Reduced membrane localization of zebrafish EGFR(C797A)-GFP following transfection into human HaCaT keratinocytes compared with wtEGFR-GFP. (*E*) Membrane:cytoplasmic GFP ratio is reduced in cells expressing EGFR(C797A) (five cells and two biological replicates, each). (*F*) Detection of EGFR sulfenylation in HEK001 human keratinocytes via Western blotting following click chemistry shows a 1.5-fold increase upon 30-min stimulation with H_2O_2. GPX serves as positive control. (*G*, *Upper*) Zoomed view of red square shown in *Lower*, *Left* image: Axon branches retract around sites of tdTomato_EGFR(C797A) expressing keratinocytes (yellow arrows), whereas axons regenerate in areas devoid of tdTomato_EGFR(C797A)$^+$ keratinocytes (white arrows). (*Lower*) Transmitted light overlay of *Upper* image in low magnification to depict the injury site. Retracting (yellow) and growing axons (white) are overlaid as 12-h tracks in the right image. (*H*) Quantification of *G* (from left: $n = 5$, 5, and 6 animals). (*I*) Axon branch number is reduced at 6 and 12 h postinjury in regions where keratinocytes express *krt4*:Gal4VP16_tdTomato_ EGFR(C797A) compared with animals in which keratinocytes express *krt4*:Gal4VP16_tdTomato. (*J*) EGFR inhibition ($n = 34$ animals) reduces HyPer oxidation compared with control animals ($n = 33$). Statistical comparisons were used as follows: (*A*, *C*, *H*, and *J*) ANOVA and Tukey's multiple-comparisons test; (*E*) Student's *t* test; (*I*) two-way ANOVA and Sidak's multiple-comparisons test.

difference at 60-mpa vehicle: 1.15 ± 0.05 vs. EGFR inhibitor: 1.032 ± 0.04, SEM) (Fig. 5*J*), suggesting that the EGFR controls H_2O_2 production under conditions of injury to sustain its activity.

EGFR-Dependent *mmp13* Expression Is Required for Axon Regeneration. We previously demonstrated with laser axotomy that cutaneous axons in the caudal fin have limited regenerative capacity in the absence of keratinocyte damage (21). Studies in

mice further showed that the uninjured epidermis stays devoid of reinnervating axons following sciatic nerve lesion (15), suggesting that cues in the extracellular matrix (ECM) of uninjured epidermis might prevent axon growth. Accordingly, skin-wounding activates MMPs (66), and thus ECM remodeling may promote growth. MMP-9 and -13 were valid candidates based on our RNA-seq data and validated qPCR (Fig. 6*A*). STRING-Db (EMBL) analysis further confirmed interactions between the EGFR and MMP-13 (Fig. 6*B*). To assess the role of MMPs in axon regeneration, we first used the MMP inhibitor, GM6001, which blocks the activity of MMP-1, -2, -3, and -9. Twelve-hour time-lapse imaging revealed that GM6001 did not significantly impair regeneration (untreated uninjured: 23.86 ± 1.2-μm untreated amputated: 83.4.9 ± 6.8 μm vs. vehicle amputated: 96.24 ± 4.6 μm vs. 10 μM GM6001 amputated: 92.33 ± 8.4 μm, SEM), suggesting that these MMPs are not involved in axon regeneration (Fig. 6*C*). To further validate this, we also used a selective MMP-9 inhibitor. This surprisingly showed that axon regeneration was significantly increased compared with vehicle controls (10 μM: 172.5 ± 23.64 μm, SEM) (Fig. 6*C* and Movie S17). Therefore, MMP-9 activity appears to restrict axon growth following tissue wounding. A strong alternative candidate mediating axon regeneration was therefore MMP-13. Twelve-hour time-lapse imaging revealed that MMP-13 inhibition with the selective MMP-13 inhibitor, DB04760, prevented axon regeneration and also induced axonal retraction, similar to *duox1* mutants and upon axonal contact with keratinocytes expressing either *gpx1a* or EGFR(C797A) (10 μM DB04760: −51.99 ± 5.8 μm [retraction]) (Fig. 6*C* and *D* and Movie S18). The antagonizing functions of MMP-9 and -13 may be necessary to coordinate tissue interactions during wound repair.

To further elucidate the relationship between EGFR, H_2O_2, and *mmp13*, we treated 3-dpf animals with either H_2O_2, the antioxidant, *N*-acetylcysteine (NAC), or EGFR inhibitor to assess H_2O_2/EGFR-dependent *mmp13a* expression via qPCR at 3 hpa. While H_2O_2 treatment significantly elevated *mmp13a* expression levels, NAC and EGFR inhibition caused significant downregulation comparable with uninjured animals (fold-change from uninjured: 0.01% H_2O_2: 5.8 ± 1.6 vs. 0.1% NAC: 1.0 ± 0.2 vs. 9 μM EGFR inhibitor: 0.9 ± 0.5, SEM) (Fig. 6*E*). This demonstrates that *mmp13a* expression is induced by H_2O_2 and EGFR following injury. We next analyzed the ECM ultrastructure surrounding cutaneous axons using transmission electron microscopy in uninjured zebrafish and following caudal fin injury in the absence and presence of DB04760. Cutaneous axons in the uninjured fin epidermis were closely associated with keratinocytes, as previously shown (67), whereas large gaps surrounded axons at 3 hpa, which was abolished in the presence of DB04760 (Fig. 6*F*). Together with evidence that MMP-13 is closely associated with cutaneous axons following caudal fin amputation (34), these data indicate that MMP-13 is recruited to sites of contact between axons and keratinocytes following injury to facilitate axon regeneration via localized matrix remodeling.

Discussion

In this study, we uncovered an H_2O_2-dependent mechanism involving EGFR oxidation and MMP-13 dependent matrix remodeling in cutaneous sensory axon regeneration following tissue wounding. We identified distinct functions for Duox1 and Nox/p22Phox in this process (Fig. 6*G*), whereby loss of *duox1* promotes axonal retraction, distinct from partial regeneration, slower Wallerian degeneration, and axonal fusion in *cyba* mutants. The slow Wallerian degeneration phenotype resembles that of Wld^S mice (68) in which a chimeric fusion between the N-terminal 70 aa of the *Ubiquitin fusion degradation protein 2a* (*Ufd2a*) and the NAD biosynthetic enzyme, *Nmnat1*, delays axon degeneration (60, 70) by inhibiting SARM1 function, which normally depletes NAD^+ following axonal injury to induce Wallerian degeneration (71–75). Wld^S transgene overexpression in *Drosophila* (76) and zebrafish (54) neurons induces the same slow-degeneration phenotype as found in mice, suggesting a conserved neuron-intrinsic mechanism. Given the protective effects of NAD^+ in injured axons, it is possible that presumptive NADPH accumulation in *cyba* mutants intersects with NAD^+ metabolism through yet unknown mechanisms. Another possibility is that NADPH accumulation protects severed axons against harmful ROS, which are most likely produced in axonal mitochondria following injury. Consistent with this idea are time-lapse imaging studies in zebrafish showing rapid mitochondrial oxidation in severed cutaneous axon fragments following axotomy, which is prevented upon Wld^S overexpression (77). Furthermore, mitochondria-specific NMNAT3 and targeted expression of Wld^S and NMNAT1 to mitochondria mimics the Wld^S phenotype (72), further implicating mitochondria in Wallerian degeneration. Thus, scavenging neuronal mitochondrial ROS may protect against Wallerian degeneration in pathologies, such as neuropathy.

The finding that severed axons fuse with intact axons upon loss of p22Phox is highly intriguing. Thus far, axonal fusion has been described only in invertebrates, such as crayfish (78), leeches (79, 80), snails (81), *Aplysia* (82), earthworms (83), and nematodes (84). Axonal fusion consists of several key events and requires that: 1) the onset of fragmentation is sufficiently delayed, 2) a molecular bridge forms between two fragments, 3) membrane fusion between two fragments establishes cytoplasmic continuity, and 4) internal structures repristinate (85, 86). Although detailed characterizations remain to be done, our time-lapse studies indicate that several key features are present in *cyba* mutants. In *Caenorhabditis elegans*, axonal fusion depends on the type I membrane protein, epithelial fusion failure 1 (EFF-1) (84), which was identified to mediate epithelial and muscle cell fusion (87). This transmembrane glycoprotein with eight predicted pairs of disulfide-linked cysteine residues has however no sequence homology in other organisms aside from *C. elegans* (87). EFF-1 was proposed to use a mechanism that combines aspects of virus-cell fusion and SNARE-mediated fusion, and thus, although EFF-1 may not be conserved, the overall fusion process may be mediated by similar fusogens in other species (88). Interestingly, Nox2 deficiency in mice has been associated with reduced SNARE-mediated glutamate release (89), indicating a cross-talk between NADPH oxidases and fusogens.

We detected more extensive H_2O_2 gradients when using HyPer imaging as compared with the narrow sulfenylation gradients formed along the wound edge detected with click chemistry and antidimedone antibody staining. Parameters such as ECM and cytoplasmic diffusion constants, and the presence of antioxidant complexes, can influence gradient formation upon localized H_2O_2 release from wound keratinocytes. H_2O_2 secretion into the extracellular space is followed by localized diffusion and entry into the cytoplasm via aquaporin channels (8, 90). Intracellular diffusion across multiple membranes appears unlikely since H_2O_2 is rapidly scavenged by intracellular antioxidant complexes. Moreover, the presence of cytoplasmic peroxiredoxins restricts H_2O_2 protein oxidation to localized areas of <1 μm diameter (27), occurring at rate constants of 10^{-5} to 10^{-8} ($M^{-1}s^{-1}$) (91, 92).

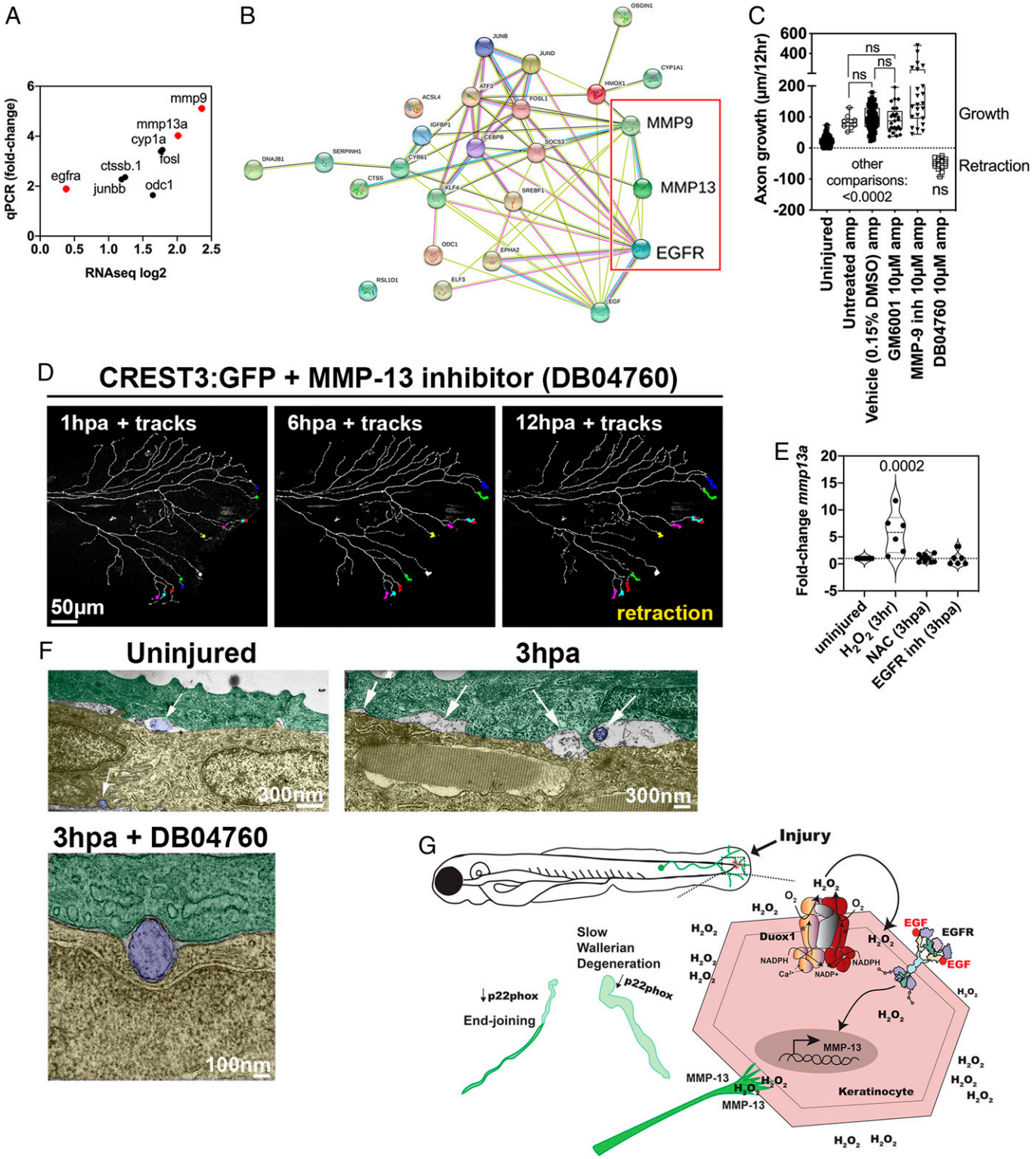

Fig. 6. EGFR promotes cutaneous axon regeneration via MMP-13 dependent ECM remodeling. (*A*) Correlation between qPCR and RNA-seq dataset shows increased *egfra* and *mmp9*, and *mmp13a* expression (red dots), among others, following H_2O_2 treatment. (*B*) String-DB shows MMP-13 interacting with the EGFR. (*C*) DB04760 but not GM6001 (MMP-1/2/3/9 inhibitor) impairs axon regeneration following injury, whereas selective MMP-9 inhibition increases regeneration (left to right: n = 13, 4, 8, 7, 6, and 4 animals). (*D*) Time-lapse sequence showing impaired axon regeneration with DB04760, with 12-h colored tracks depicting axonal retraction (Movie S18). (*E*) qPCR shows increased *mmp13a* expression following 3-h H_2O_2 treatment. *mmp13a* expression is abolished at 3 hpa upon treatment with the antioxidant, NAC, and EGFR inhibitor (n = 3 biological replicates with 10 pooled 3-dpf zebrafish each). Statistical comparison with uninjured control group is shown. (*F*) Transmission electron microscopy at 3 hpa shows large gaps between keratinocytes (periderm = green, basal layer = yellow, axons = blue) at sites harboring axon branches. Gaps are absent in uninjured epidermis and following treatment with DB04760. (*G*) Model shows dual H_2O_2 functions in keratinocytes leading to EGFR oxidation and MMP-13 activation mediating axon growth within the epidermis. Loss of neuron-intrinsic p22Phox slows Wallerian degeneration and promotes axonal fusion mediated. Statistical comparisons in *C* and *E* used one-way ANOVA and Bonferroni's posttest.

Consistently, mathematical modeling predicted that extracellular H_2O_2 can overcome distances of ~30 μm with antioxidant barriers (93), which is one to two cell diameters, similar to the sulfenylation gradient. The difference in gradient detection may therefore relate to 1) HyPer overexpression within cells, which can detect even minute amounts of H_2O_2 entering the cell, and 2) low sensitivity of experimental detection of sulfenylation detection methods that is perpetuated by a relatively low abundance of endogenous proteins available for peroxiredoxin-dependent thiolation.

Our study suggests that oxidation-dependent EGFR activation parallels that in cancer cells (28), consistent with the idea that cancers represent nonhealing wounds (94, 95). Although this comparison has referred to chronic inflammatory processes, our data indicate that other mechanisms occur similarly, such as oxidative activation of the EGFR, which does not involve the immune system. Increased attention has been given in the past decade to interactions between neurons and tumors (96–98). An intriguing possibility may therefore be that oxidation-dependent EGFR activation stimulates nerve innervation of tumors to promote growth, which remains to be elucidated.

We have demonstrated distinct functions for MMP-9 and MMP-13 in cutaneous axon regeneration, whereby MMP-9 serves a modulatory role that restrains axon growth. This restraining activity may be indirectly regulated through cleavage of membrane-tethered glycoproteins. For example, following spinal cord injury, MMP-9 cleaves growth-inhibitory myelin associated glycoprotein (MAG) fragments that have been associated with axon growth prevention, which can be circumvented upon MMP-9 inhibition (99). A similar mechanism in the epidermis may reduce axon regeneration following tissue injury, possibly to coordinate tissue repair processes. Alternatively, MMP-9 inhibition may reduce environmental constraints that would otherwise allow axons to regrow more rapidly. For example, MMP-9–null mice show defects in epidermal keratinocyte migration (100). A similar function in zebrafish could create a more permissive axon growth environment.

Materials and Methods

Zebrafish Husbandry and Transgenic Lines. For wild-type strains, zebrafish (Nacre/*mitfa*) and AB strains were purchased from the Zebrafish International Resource Centre. Embryos were raised and bred according to NIH guidelines. Animals were handled in strict accordance with good animal practices as approved by the appropriate institutional Animal Care and Use Committee (IACUC) (University of Miami's #A-3224-01 and Association for Assessment and Accreditation of Laboratory Animal Care accreditation site: 001069; MDI Biological Laboratory IACUC #A13-20). Zebrafish eggs were incubated at 28.5 °C in a 14:10-h light:dark cycle.

Pharmacological Agents. The following inhibitors and concentrations were added 2 h prior to imaging (unless stated otherwise in the text) and kept in the solution during imaging unless otherwise stated: DMSO vehicle (0.15%); *Phluroglucinol* (25 μM; Sigma-Aldrich, Cat. no. 79330); 5,5-dimethyl-1,3-cyclohexanedion, *dimedone* (1.5 mM; Sigma-Aldrich, Cat. no. D153303). Dimedone selectively and irreversibly binds to sulfenic acid (26) and was added 1 h prior to and 30 min after amputation. Click-Tag DYn-2 (10 μM; Cayman Chemical, Cat. no. 11220); EGFR inhibitor (8 and 10 μM; Cayman Chemical, Cat. no. 16363); Erbstatin (10 μM; Cayman Chemical, Cat. no.10010238); Lavendustin A (10 μM; EMD Millipore, Cat. no. 428150); Tyrphostin A23 (10 μM; Sigma-Aldrich, Cat. no. T7165); actinomycin D (10 μM; Tocris, Cat. no. 1229); 6-MP (10 μM; Sigma-Aldrich, Cat. no. 38171); DRB (10 μM; Cayman Chemical, Cat. no. 10010302); cycloheximide (10 μM; Cayman Chemical, Cat. no. 14126); hydrogen peroxide (0.01% and 0.3%; Sigma-Aldrich, Cat. no. H1009); GM6001 (10 μM; Ilomastat, Millipore Sigma, Cat. no. CC1100); DB04760 (MMP-13 inhibitor, Millipore Sigma, Cat. No. 444283); NF-κB inhibitor (10 μM; JSH-23, Sigma-Aldrich, Cat. no. J4455). MMP-9 inhibitor I (Cayman Chemical, Cat. no.15942).

Image Processing. Images were processed and analyzed in Imaris (Bitplane) and Fiji. HyPer maximum intensity projections were generated in ZEN (Zeiss). The ratiometric view for each image was created using the Image Calculator in ZEN with the following formula: (488 nm/405 nm) × 1,500 for keratinocytes and (488 nm/405 nm) × 1,200 for axons and Spectrum LUT. For publication, projected tiffs were processed in Photoshop. Three-dimensional reconstructions were performed in Imaris using the semiautomated Surfaces feature. Schematics were prepared in Adobe Illustrator and Microsoft PowerPoint.

Statistical Analyses. Statistical comparisons were made using Prism 7-9 (GraphPad). Comparisons of two groups was done using Student's *t* test. Comparisons by more than two groups and a single variable were done using one-way ANOVA, whereas comparisons of multiple groups and variables were done using two-way ANOVA. All comparisons were performed at $\alpha = 0.05$ (95% confidence interval), using multiple comparisons posttests, as indicated in figure legends. The SEM is shown for all experiments where at least two biological replicates were used per group.

Data Availability. All study data are included in the main text and supporting information.

ACKNOWLEDGMENTS. We thank Dr. Alvaro Sagasti (University of California, Los Angeles) and Dr. Kate Carroll (Scripps Institute) for reagents, and Ricardo Cepeda and Dr. Julia Dallman for zebrafish maintenance. S.R. was funded by grants P20GM104318, 1R01CA215973, and P20GM103423. M.Y. was supported by grant P20GM103423.

Author affiliations: [a]Department of Biology, University of Miami, Coral Gables, FL 33146; [b]Department of Regenerative Biology and Medicine, MDI Biological Laboratory, Bar Harbor, ME 04672; and [c]Sylvester Comprehensive Cancer Center, Miller School of Medicine, Miami, FL 33136

1. M. Guida *et al.*, Nuclear Nox4-derived reactive oxygen species in myelodysplastic syndromes. *BioMed Res. Int.* **2014**, 456937 (2014).
2. F. R. Laurindo, T. L. Araujo, T. B. Abrahão, Nox NADPH oxidases and the endoplasmic reticulum. *Antioxid. Redox Signal.* **20**, 2755–2775 (2014).
3. J. D. Van Buul, M. Fernandez-Borja, E. C. Anthony, P. L. Hordijk, Expression and localization of NOX2 and NOX4 in primary human endothelial cells. *Antioxid. Redox Signal.* **7**, 308–317 (2005).
4. A. Donkó, Z. Péterfi, A. Sum, T. Leto, M. Geiszt, Dual oxidases. *Philos. Trans. R. Soc. Lond. B Biol. Sci.* **360**, 2301–2308 (2005).
5. Y. Nisimoto, B. A. Diebold, D. Cosentino-Gomes, J. D. Lambeth, Nox4: A hydrogen peroxide-generating oxygen sensor. *Biochemistry* **53**, 5111–5120 (2014).
6. K. Bedard, K. H. Krause, The NOX family of ROS-generating NADPH oxidases: Physiology and pathophysiology. *Physiol. Rev.* **87**, 245–313 (2007).
7. A. Panday, M. K. Sahoo, D. Osorio, S. Batra, NADPH oxidases: An overview from structure to innate immunity-associated pathologies. *Cell. Mol. Immunol.* **12**, 5–23 (2015).
8. G. P. Bienert *et al.*, Specific aquaporins facilitate the diffusion of hydrogen peroxide across membranes. *J. Biol. Chem.* **282**, 1183–1192 (2007).
9. A. Hall, D. Parsonage, L. B. Poole, P. A. Karplus, Structural evidence that peroxiredoxin catalytic power is based on transition-state stabilization. *J. Mol. Biol.* **402**, 194–209 (2010).
10. R. Brigelius-Flohé, L. Flohé, Basic principles and emerging concepts in the redox control of transcription factors. *Antioxid. Redox Signal.* **15**, 2335–2381 (2011).
11. A. V. Peskin *et al.*, Modifying the resolving cysteine affects the structure and hydrogen peroxide reactivity of peroxiredoxin 2. *J. Biol. Chem.* **296**, 100494 (2021).
12. Y. Liu *et al.*, NRF2 signalling pathway: New insights and progress in the field of wound healing. *J. Cell. Mol. Med.* **25**, 5857–5868 (2021).
13. I. Süntar *et al.*, Regulatory role of Nrf2 signaling pathway in wound healing process. *Molecules* **26**, 2424 (2021).
14. A. Hervera *et al.*, Reactive oxygen species regulate axonal regeneration through the release of exosomal NADPH oxidase 2 complexes into injured axons. *Nat. Cell Biol.* **20**, 307–319 (2018).
15. X. Navarro, E. Verdú, G. Wendelschafer-Crabb, W. R. Kennedy, Immunohistochemical study of skin reinnervation by regenerative axons. *J. Comp. Neurol.* **380**, 164–174 (1997).
16. R. Mackel, E. Kunesch, F. Waldhör, A. Struppler, Reinnervation of mechanoreceptors in the human glabrous skin following peripheral nerve repair. *Brain Res.* **268**, 49–65 (1983).
17. M. Reynolds, D. Alvares, J. Middleton, M. Fitzgerald, Neonatally wounded skin induces NGF-independent sensory neurite outgrowth in vitro. *Brain Res. Dev. Brain Res.* **102**, 275–283 (1997).
18. M. L. Reynolds, M. Fitzgerald, Long-term sensory hyperinnervation following neonatal skin wounds. *J. Comp. Neurol.* **358**, 487–498 (1995).
19. S. Harsum, J. D. Clarke, P. Martin, A reciprocal relationship between cutaneous nerves and repairing skin wounds in the developing chick embryo. *Dev. Biol.* **238**, 27–39 (2001).
20. M. Mihara, Regenerated cutaneous nerves in human epidermal and subepidermal regions. An electron microscopy study. *Arch. Dermatol. Res.* **276**, 115–122 (1984).

21. S. Rieger, A. Sagasti, Hydrogen peroxide promotes injury-induced peripheral sensory axon regeneration in the zebrafish skin. *PLoS Biol.* **9**, e1000621 (2011).
22. K. Xu, F. S. Yu, Impaired epithelial wound healing and EGFR signaling pathways in the corneas of diabetic rats. *Invest. Ophthalmol. Vis. Sci.* **52**, 3301–3308 (2011).
23. T. S. Lisse, S. Rieger, IKKα regulates human keratinocyte migration through surveillance of the redox environment. *J. Cell Sci.* **130**, 975–988 (2017).
24. L. A. Hansen *et al.*, Genetically null mice reveal a central role for epidermal growth factor receptor in the differentiation of the hair follicle and normal hair development. *Am. J. Pathol.* **150**, 1959–1975 (1997).
25. S. K. Repertinger *et al.*, EGFR enhances early healing after cutaneous incisional wounding. *J. Invest. Dermatol.* **123**, 982–989 (2004).
26. S. E. Leonard, K. G. Reddie, K. S. Carroll, Mining the thiol proteome for sulfenic acid modifications reveals new targets for oxidation in cells. *ACS Chem. Biol.* **4**, 783–799 (2009).
27. R. D. M. Travasso, F. Sampaio Dos Aidos, A. Bayani, P. Abranches, A. Salvador, Localized redox relays as a privileged mode of cytoplasmic hydrogen peroxide signaling. *Redox Biol.* **12**, 233–245 (2017).
28. C. E. Paulsen *et al.*, Peroxide-dependent sulfenylation of the EGFR catalytic site enhances kinase activity. *Nat. Chem. Biol.* **8**, 57–64 (2011).
29. P. Niethammer, C. Grabher, A. T. Look, T. J. Mitchison, A tissue-scale gradient of hydrogen peroxide mediates rapid wound detection in zebrafish. *Nature* **459**, 996–999 (2009).
30. S. Isogai, M. Horiguchi, B. M. Weinstein, The vascular anatomy of the developing zebrafish: An atlas of embryonic and early larval development. *Dev. Biol.* **230**, 278–301 (2001).
31. S. K. Yoo, T. W. Starnes, Q. Deng, A. Huttenlocher, Lyn is a redox sensor that mediates leukocyte wound attraction in vivo. *Nature* **480**, 109–112 (2011).
32. M. Lo Conte, K. S. Carroll, The redox biochemistry of protein sulfenylation and sulfinylation. *J. Biol. Chem.* **288**, 26480–26488 (2013).
33. V. V. Belousov *et al.*, Genetically encoded fluorescent indicator for intracellular hydrogen peroxide. *Nat. Methods* **3**, 281–286 (2006).
34. T. S. Lisse *et al.*, Paclitaxel-induced epithelial damage and ectopic MMP-13 expression promotes neurotoxicity in zebrafish. *Proc. Natl. Acad. Sci. U.S.A.* **113**, E2189–E2198 (2016).
35. M. I. Koster, D. R. Roop, p63 and epithelial appendage development. *Differentiation* **72**, 364–370 (2004).
36. S. K. Yoo, C. M. Freisinger, D. C. LeBert, A. Huttenlocher, Early redox, Src family kinase, and calcium signaling integrate wound responses and tissue regeneration in zebrafish. *J. Cell Biol.* **199**, 225–234 (2012).
37. Y. H. Seo, K. S. Carroll, Quantification of protein sulfenic acid modifications using isotope-coded dimedone and iododimedone. *Angew. Chem. Int. Ed. Engl.* **50**, 1342–1345 (2011).
38. R. D. Michalek *et al.*, The requirement of reversible cysteine sulfenic acid formation for T cell activation and function. *J. Immunol.* **179**, 6456–6467 (2007).
39. B. Quéguineur *et al.*, Phloroglucinol: Antioxidant properties and effects on cellular oxidative markers in human HepG2 cell line. *Food Chem. Toxicol.* **50**, 2886–2893 (2012).
40. M. V. Flores *et al.*, Dual oxidase in the intestinal epithelium of zebrafish larvae has anti-bacterial properties. *Biochem. Biophys. Res. Commun.* **400**, 164–168 (2010).
41. S. Hirakawa, R. Saito, H. Ohara, R. Okuyama, S. Aiba, Dual oxidase 1 induced by Th2 cytokines promotes STAT6 phosphorylation via oxidative inactivation of protein tyrosine phosphatase 1B in human epidermal keratinocytes. *J. Immunol.* **186**, 4762–4770 (2011).
42. H. Sumimoto, Structure, regulation and evolution of nox-family NADPH oxidases that produce reactive oxygen species. *FEBS J.* **275**, 3249–3277 (2008).
43. C. J. Weaver, Y. F. Leung, D. M. Suter, Expression dynamics of NADPH oxidases during early zebrafish development. *J. Comp. Neurol.* **524**, 2130–2141 (2016).
44. E. Duregotti *et al.*, Mitochondrial alarmins released by degenerating motor axon terminals activate perisynaptic Schwann cells. *Proc. Natl. Acad. Sci. U.S.A.* **112**, E497–E505 (2015).
45. G. W. Stuart, J. V. McMurray, M. Westerfield, Replication, integration and stable germ-line transmission of foreign sequences injected into early zebrafish embryos. *Development* **103**, 403–412 (1988).
46. Y. Yamanashi *et al.*, Selective expression of a protein-tyrosine kinase, p56lyn, in hematopoietic cells and association with production of human T-cell lymphotropic virus type I. *Proc. Natl. Acad. Sci. U.S.A.* **86**, 6538–6542 (1989).
47. E. Yamada, J. E. Pessin, I. J. Kurland, G. J. Schwartz, C. C. Bastie, Fyn-dependent regulation of energy expenditure and body weight is mediated by tyrosine phosphorylation of LKB1. *Cell Metab.* **11**, 113–124 (2010).
48. H. Umemori *et al.*, Specific expressions of Fyn and Lyn, lymphocyte antigen receptor-associated tyrosine kinases, in the central nervous system. *Brain Res. Mol. Brain Res.* **16**, 303–310 (1992).
49. H. S. Lee *et al.*, Src tyrosine kinases mediate activations of NF-kappaB and integrin signal during lipopolysaccharide-induced acute lung injury. *J. Immunol.* **179**, 7001–7011 (2007).
50. G. Gloire, S. Legrand-Poels, J. Piette, NF-kappaB activation by reactive oxygen species: Fifteen years later. *Biochem. Pharmacol.* **72**, 1493–1505 (2006).
51. J. R. Scott, P. Muangman, N. S. Gibran, Making sense of hypertrophic scar: A role for nerves. *Wound Repair Regen.* **15** (suppl. 1), S27–S31 (2007).
52. M. J. Stasia, CYBA encoding p22(phox), the cytochrome b558 alpha polypeptide: Gene structure, expression, role and physiopathology. *Gene* **586**, 27–35 (2016).
53. M. F. Lyon, B. W. Ogunkolade, M. C. Brown, D. J. Atherton, V. H. Perry, A gene affecting Wallerian nerve degeneration maps distally on mouse chromosome 4. *Proc. Natl. Acad. Sci. U.S.A.* **90**, 9717–9720 (1993).
54. S. M. Martin, G. S. O'Brien, C. Portera-Cailliau, A. Sagasti, Wallerian degeneration of zebrafish trigeminal axons in the skin is required for regeneration and developmental pruning. *Development* **137**, 3985–3994 (2010).
55. B. Neumann, K. C. Nguyen, D. H. Hall, A. Ben-Yakar, M. A. Hilliard, Axonal regeneration proceeds through specific axonal fusion in transected C. elegans neurons. *Dev. Dyn.* **240**, 1365–1372 (2011).
56. J. Aoi *et al.*, Angiopoietin-like protein 2 accelerates carcinogenesis by activating chronic inflammation and oxidative stress. *Mol. Cancer Res.* **12**, 239–249 (2014).
57. C. C. Toth *et al.*, Locally synthesized calcitonin gene-related peptide has a critical role in peripheral nerve regeneration. *J. Neuropathol. Exp. Neurol.* **68**, 326–337 (2009).
58. H. Jung, B. C. Yoon, C. E. Holt, Axonal mRNA localization and local protein synthesis in nervous system assembly, maintenance and repair. *Nat. Rev. Neurosci.* **13**, 308–324 (2012).
59. P. K. Sahoo *et al.*, Axonal G3BP1 stress granule protein limits axonal mRNA translation and nerve regeneration. *Nat. Commun.* **9**, 3358 (2018).
60. T. S. Lisse, B. L. King, S. Rieger, Comparative transcriptomic profiling of hydrogen peroxide signaling networks in zebrafish and human keratinocytes: Implications toward conservation, migration and wound healing. *Sci. Rep.* **6**, 20328 (2016).
61. A. Maklad *et al.*, The EGFR is required for proper innervation to the skin. *J. Invest. Dermatol.* **129**, 690–698 (2009).
62. H. Umezawa *et al.*, Studies on a new epidermal growth factor-receptor kinase inhibitor, erbstatin, produced by MH435-hF3. *J. Antibiot. (Tokyo)* **39**, 170–173 (1986).
63. Q. Zhang *et al.*, Discovery of EGFR selective 4,6-disubstituted pyrimidines from a combinatorial kinase-directed heterocycle library. *J. Am. Chem. Soc.* **128**, 2182–2183 (2006).
64. N. Godin-Heymann *et al.*, Oncogenic activity of epidermal growth factor receptor kinase mutant alleles is enhanced by the T790M drug resistance mutation. *Cancer Res.* **67**, 7319–7326 (2007).
65. T. Truong, K. Carroll, Bioorthogonal chemical reporters for analyzing protein sulfenylation in cells. *Curr. Protoc. Chem. Biol.* **4**, 101–122 (2012).
66. N. Hattori *et al.*, MMP-13 plays a role in keratinocyte migration, angiogenesis, and contraction in mouse skin wound healing. *Am. J. Pathol.* **175**, 533–546 (2009).
67. G. S. O'Brien *et al.*, Coordinate development of skin cells and cutaneous sensory axons in zebrafish. *J. Comp. Neurol.* **520**, 816–831 (2012).
68. E. R. Lunn, V. H. Perry, M. C. Brown, H. Rosen, S. Gordon, Absence of Wallerian degeneration does not hinder regeneration in peripheral nerve. *Eur. J. Neurosci.* **1**, 27–33 (1989).
69. L. Conforti *et al.*, A Ufd2/D4Cole1e chimeric protein and overexpression of Rbp7 in the slow Wallerian degeneration (WldS) mouse. *Proc. Natl. Acad. Sci. U.S.A.* **97**, 11377–11382 (2000).
70. T. G. Mack *et al.*, Wallerian degeneration of injured axons and synapses is delayed by a Ube4b/Nmnat chimeric gene. *Nat. Neurosci.* **4**, 1199–1206 (2001).
71. J. Gerdts, D. W. Summers, J. Milbrandt, A. DiAntonio, Axon self-destruction: New links among SARM1, MAPKs, and NAD+ metabolism. *Neuron* **89**, 449–460 (2016).
72. E. Babetto *et al.*, Targeting NMNAT1 to axons and synapses transforms its neuroprotective potency in vivo. *J. Neurosci.* **30**, 13291–13304 (2010).
73. Y. Sasaki, B. P. Vohra, R. H. Baloh, J. Milbrandt, Transgenic mice expressing the Nmnat1 protein manifest robust delay in axonal degeneration in vivo. *J. Neurosci.* **29**, 6526–6534 (2009).
74. Y. Sasaki, J. Milbrandt, Axonal degeneration is blocked by nicotinamide mononucleotide adenylyltransferase (Nmnat) protein transduction into transected axons. *J. Biol. Chem.* **285**, 41211–41215 (2010).
75. J. Gilley, M. P. Coleman, Endogenous Nmnat2 is an essential survival factor for maintenance of healthy axons. *PLoS Biol.* **8**, e1000300 (2010).
76. E. D. Hoopfer *et al.*, Wlds protection distinguishes axon degeneration following injury from naturally occurring developmental pruning. *Neuron* **50**, 883–895 (2006).
77. K. C. O'Donnell, M. E. Vargas, A. Sagasti, WldS and PGC-1α regulate mitochondrial transport and oxidation state after axonal injury. *J. Neurosci.* **33**, 14778–14790 (2013).
78. R. R. Hoy, G. D. Bittner, D. Kennedy, Regeneration in crustacean motoneurons: Evidence for axonal fusion. *Science* **156**, 251–252 (1967).
79. S. A. Deriemer, E. J. Elliott, E. R. Macagno, K. J. Muller, Morphological evidence that regenerating axons can fuse with severed axon segments. *Brain Res.* **272**, 157–161 (1983).
80. E. Frank, J. K. Jansen, E. Rinvik, A multisomatic axon in the central nervous system of the leech. *J. Comp. Neurol.* **159**, 1–13 (1975).
81. A. D. Murphy, S. B. Kater, Specific reinnervation of a target organ by a pair of identified molluscan neurons. *Brain Res.* **156**, 322–328 (1978).
82. S. S. Bedi, D. L. Glanzman, Axonal rejoining inhibits injury-induced long-term changes in Aplysia sensory neurons in vitro. *J. Neurosci.* **21**, 9667–9677 (2001).
83. S. C. Birse, G. D. Bittner, Regeneration of giant axons in earthworms. *Brain Res.* **113**, 575–581 (1976).
84. A. Ghosh-Roy, Z. Wu, A. Goncharov, Y. Jin, A. D. Chisholm, Calcium and cyclic AMP promote axonal regeneration in Caenorhabditis elegans and require DLK-1 kinase. *J. Neurosci.* **30**, 3175–3183 (2010).
85. B. Neumann, C. Linton, R. Giordano-Santini, M. A. Hilliard, Axonal fusion: An alternative and efficient mechanism of nerve repair. *Prog. Neurobiol.* **173**, 88–101 (2019).
86. B. Neumann, M. A. Hilliard, Axonal repair by fusion: Pitfalls, consequences and solutions. *FASEB J.* **33**, 13071–13074 (2019).
87. W. A. Mohler *et al.*, The type I membrane protein EFF-1 is essential for developmental cell fusion. *Dev. Cell* **2**, 355–362 (2002).
88. N. G. Brukman, B. Uygur, B. Podbilewicz, L. V. Chernomordik, How cells fuse. *J. Cell Biol.* **218**, 1436–1451 (2019).
89. Z. Wang *et al.*, NOX2 deficiency ameliorates cerebral injury through reduction of complexin II-mediated glutamate excitotoxicity in experimental stroke. *Free Radic. Biol. Med.* **65**, 942–951 (2013).
90. G. P. Bienert, J. K. Schjoerring, T. P. Jahn, Membrane transport of hydrogen peroxide. *Biochim. Biophys. Acta* **1758**, 994–1003 (2006).
91. F. M. Low, M. B. Hampton, A. V. Peskin, C. C. Winterbourn, Peroxiredoxin 2 functions as a noncatalytic scavenger of low-level hydrogen peroxide in the erythrocyte. *Blood* **109**, 2611–2617 (2007).
92. B. Manta *et al.*, The peroxidase and peroxynitrite reductase activity of human erythrocyte peroxiredoxin 2. *Arch. Biochem. Biophys.* **484**, 146–154 (2009).
93. M. Jelcic, B. Enyedi, J. B. Xavier, P. Niethammer, Image-based measurement of H_2O_2 reaction-diffusion in wounded Zebrafish larvae. *Biophys. J.* **112**, 2011–2018 (2017).
94. S. A. Eming, T. Krieg, J. M. Davidson, Inflammation in wound repair: Molecular and cellular mechanisms. *J. Invest. Dermatol.* **127**, 514–525 (2007).
95. M. Schäfer, S. Werner, Cancer as an overhealing wound: An old hypothesis revisited. *Nat. Rev. Mol. Cell Biol.* **9**, 628–638 (2008).
96. A. Kamiya *et al.*, Genetic manipulation of autonomic nerve fiber innervation and activity and its effect on breast cancer progression. *Nat. Neurosci.* **22**, 1289–1305 (2019).
97. M. J. Szpunar, E. K. Belcher, R. P. Dawes, K. S. Madden, Sympathetic innervation, norepinephrine content, and norepinephrine turnover in orthotopic and spontaneous models of breast cancer. *Brain Behav. Immun.* **53**, 223–233 (2016).
98. M. Austin, L. Elliott, N. Nicolaou, A. Grabowska, R. P. Hulse, Breast cancer induced nociceptor aberrant growth and collateral sensory axonal branching. *Oncotarget* **8**, 76606–76621 (2017).
99. V. I. Shubayev, A. Y. Strongin, Tissue inhibitors of metalloproteases strike a nerve. *Neural Regen. Res.* **13**, 1890–1892 (2018).
100. T. R. Kyriakides *et al.*, Mice that lack matrix metalloproteinase-9 display delayed wound healing associated with delayed reepithelization and disordered collagen fibrillogenesis. *Matrix Biol.* **28**, 65–73 (2009).